Mechanism of Inducible Nitric Oxide Synthase Inactivation by Aminoguanidine and L-N^6-(1-Iminoethyl)lysine†

Ruslana Bryk* and Donald J. Wolff

Department of Pharmacology, University of Medicine and Dentistry of New Jersey, Robert Wood Johnson Medical School, Piscataway, New Jersey 08854

Received August 20, 1997; Revised Manuscript Received November 13, 1997

ABSTRACT: The inducible nitric oxide synthase (iNOS) selective inhibitors aminoguanidine (AG) and N^6-(1-iminoethyl)-L-lysine (NIL), under conditions that support catalytic turnover, inactivate the enzyme by altering in different ways the functionality of the active site. NIL inactivation of the iNOS primarily targets the heme residue at the active site, as evidenced by a time- and concentration-dependent loss of heme fluorescence that accompanies the loss of NO-forming activity. The NIL-inactivated iNOS dimers that have lost their heme partially disassemble into monomers with no fluorometrically detectable heme. AG inactivation of the iNOS is not accompanied by heme destruction, as evidenced by retention of heme fluorescence and absorbance after complete loss of NO-forming activity. The AG-inactivated iNOS dimers do not disassemble into monomers as extensively as NIL-inactivated dimers. Incubation of the iNOS with ^{14}C-labeled NIL results in no detectable protein-associated radioactivity in the NIL-inactivated iNOS, suggesting that the primary mechanism of the iNOS inactivation by NIL is heme alteration and loss. In contrast, incubations of iNOS with ^{14}C-labeled AG result in the incorporation of radioactivity into both iNOS protein and low molecular weight structures that migrate by SDS−PAGE similarly to free heme. These observations suggest that AG inactivation proceeds through multiple pathways of covalent modification of the iNOS protein and the heme residue at the active site, but which sustain the integrity of the heme porphyrin ring.

Nitric oxide synthase (NOS)[1] catalyzes the formation of nitric oxide (NO) and citrulline from the amino acid L-arginine (*1*). The enzyme contains two functional domains and is a self-sufficient cytochrome P-450-like system with reductase and oxygenase domains within a single polypeptide chain (*2*). The C-terminal reductase domain transfers electrons from NADPH to FAD and FMN and communicates with the N-terminal oxygenase domain through a centrally located calmodulin-binding domain. Upon calmodulin binding, the interdomain flow of electrons is enabled. The N-terminal oxygenase domain forms the active site and contains binding sites for L-arginine, tetrahydrobiopterin (BH_4), and iron protoporphyrin IX (heme), which is coordinated through a cysteine thiol group and accepts electrons from the reductase domain (*3*).

The inducible NOS is the Ca^{2+}-independent, transcriptionally regulated isoform and is involved in protective mechanisms of host defense being induced during infection and in chronic inflammation (*4*). NO produced by the iNOS, though very important as a physiological mediator, is apparently extremely cytotoxic if produced in excess, contributing to the profound cellular damage observed in a number of pathological conditions. Thus, the hypotensive crisis of septic shock and the extensive cellular damage observed in autoimmune disorders such as rheumatoid arthritis and multiple sclerosis are associated with the generation of NO mediated by the iNOS isoform (*5*). Therefore, selective pharmacological inhibition of NOS isoforms is envisioned as a new therapeutic strategy in the treatment of diverse clinical conditions and pathological disorders.

Aminoguanidine and N^6-(1-iminoethyl)-L-lysine have been identified as two relatively selective iNOS inhibitors that show promise of clinical utility (*6*−*8*). Though widely studied in experimental models, the exact molecular and chemical mechanisms for their inhibition and selectivity toward the iNOS isoform are unknown. Both compounds inhibit NO and citrulline production by NOS isoforms as well as the substrate-independent NADPH-oxidase activity without affecting cytochrome *c* reductase activity (*9*, unpublished results). NIL and AG are competitive versus L-arginine and produce a time-dependent inactivation of the citrulline- and NO-forming activity of iNOS only in the presence of the cosubstrates NADPH and oxygen necessary to support catalytic activity, thus satisfying criteria for mechanism-based inactivators that should be processed by an enzyme to their reactive intermediates during its normal catalytic cycle (*10*). The intermediate compound formed

† This work was supported by National Institute of Health Grants HL 54768 and ES 06897.

* Corresponding author. Tel: (732)-235-4087. Fax: (732)-235-4073. E-mail: bryk@umdnj.edu.

[1] Abbreviations: iNOS, inducible nitric oxide synthase; NO, nitric oxide; AG, aminoguanidine; NIL, N^6-(1-iminoethyl)-L-lysine; NMA, N^G-methyl-L-arginine; BH_4, (6*R*)-5,6,7,8-tetrahydro-L-biopterin; NADPH, nicotinamide adenine dinucleotide phosphate, reduced form; FAD, flavin adenine dinucleotide; FMN, flavin mononucleotide; LPS, lipopolysaccharide; HPLC, high-pressure liquid chromatography; SDS−PAGE, sodium dodecyl sulfate−polyacrylamide gel electrophoresis; DTT, dithiothrietol; EGTA, ethylene glycol bis(β-aminoethyl ether) *N*,*N*,*N*′,*N*′-tetraacetic acid; HEPES, *N*-(2-hydroxyethyl)piperazine-*N*′-2-ethanesulfonic acid; TFA, trifluoroacetic acid.

S0006-2960(97)02065-5 CCC: $15.00 © 1998 American Chemical Society
Published on Web 03/17/1998

from these alternate substrates is highly reactive, often a free radical, which by attacking an active site "target" covalently modifies it, thereby irreversibly inactivating the enzyme. Studies of mechanism-based inhibitors of the cytochromes P-450 have been performed and have established three major pathways for inactivation that include covalent modification of the heme residue at the active site, covalent modification of the protein chain and covalent linkage of a modified heme residue to the protein at the active site (*11*).

No studies concerning the detailed molecular mechanism of the iNOS inactivation by either AG or NIL are available. In this manuscript we report our findings regarding molecular pathways of iNOS inactivation by the two mechanism-based inhibitors AG and NIL.

MATERIALS AND METHODS

Materials. [^{14}C]-Aminoguanidine (56 mCi/mmol) and [^{14}C(U)]-L-N^6-(1-iminoethyl)lysine (300 mCi/mmol) were custom synthesized by Moravek Biochemicals, Inc. L-[2,3-^{3}H]Arginine (40−70 Ci/mmol) was purchased from New England Nuclear. Murine (γ-interferon) was obtained from Genzyme. Rabbit polyclonal anti-iNOS antibodies were from Upstate Biotechnology Inc. BH_4 was purchased from Dr. B. Schircks Laboratories (Jona, Switzerland). All other reagents were from Sigma.

Purification of iNOS. Inducible NOS was prepared from murine RAW 264.7 macrophages induced overnight with 5 μg/mL LPS and 50 units/mL mouse γ-interferon. Cells were homogenized in five volumes of homogenization buffer (HB) containing 50 mM MOPS, pH 7.4, 1 mM EGTA, 1 mM DTT, 100 mM NaCl, 0.5% CHAPSO, 10% glycerol, 25 μM L-arginine, 100 μM BH_4, 1 mM PMSF, 20 μg/mL leupeptin, and 100 μg/mL Bowman-Birk protease inhibitor (*12*). Lysates were centrifuged at 12000*g*, and the supernate was adjusted to contain 0.05 μmol of 2′,5′-ADP-agarose/mL and rocked for 40 min at 4 °C. The resin was washed with 500 mM NaCl and the iNOS eluted with HB containing 5 mM NADPH. The affinity-purified iNOS prepared this way yielded a preparation that was highly enriched in the iNOS protein, as judged by the SDS−PAGE. All of the heme in the preparation was exclusively associated with the iNOS protein, as determined by cofractionation of the heme absorbance at 398 nm and/or fluorescence at 605 nm (excitation 410 nm) with the citrulline-forming activity of the iNOS during HPLC gel filtration on the TSK Progel G3000 SWXL (Supelco) column (data not shown) and in sucrose density gradient fractionation. Thus, the iNOS protein represented a single major hemoprotein of the affinity-purified preparation supported also by complete precipitation of the heme fluorescence during iNOS immunoprecipitation with anti-iNOS antibodies (data not shown). The enzyme was stored in aliquots in 10% glycerol and 100 μM BH_4 at −70 °C.

The affinity-purified preparation of the iNOS was further purified to homogeneity on DE-cellulose (Whatman) equilibrated in HB containing 50 mM NaCl. A portion of the affinity-purified iNOS eluted from the 2′,5′-ADP-agarose was immediately applied to DE-cellulose, the resin was washed with HB containing 100 mM NaCl, and the iNOS was eluted with HB containing 250 mM NaCl. The eluate was concentrated in a Centricon 100 (Amicon) concentrating device and appeared to be 95% homogeneous, as determined by silver-stained SDS−PAGE (data not shown).

iNOS Incubations with Inhibitors. Incubations were carried out in a total volume of 1−2 mL containing 100 μM NADPH, 100 μM BH_4, and 1−5 μM iNOS in 50 mM HEPES, pH 7.5, and were initiated by the addition of an inhibitor. Reaction mixtures were incubated for 2−3 h at 30 °C until no activity was detected in the citrulline or NO formation assays. In the incubations with ^{14}C-labeled inhibitors, the reaction mixtures were run through multiple cycles of concentration and dilution in a Centricon 30 device (Amicon) in order to remove the free unreacted inhibitor when necessary.

Citrulline Formation Assay. Citrulline formation by iNOS was assayed in 150 μL reaction mixtures containing 30 mM Hepes, pH 7.5, 1 mM DTT, 120 nM L-[2,3-^{3}H]arginine, 1 mM EGTA, 100 μM NADPH, and 300 μM BH_4. Incubations were initiated by the addition of enzyme and reaction mixtures incubated for 30 min at 30 °C in duplicate and reactions stopped as described by Wolff and Datto (*13*).

Cytochrome c Reductase Assay. Cytochrome *c* reductase activity was measured spectrophotometrically by the change in absorbance at 550 nm using a Shimadzu UV-160A spectrophotometer. Reaction mixtures contained 100 mM Hepes, pH 7.5, 1 mM EGTA, 100 μM NADPH, and 50 μM cytochrome *c* in a total volume of 1 mL, and incubations were initiated by the addition of enzyme sample and were carried out for 30 min at 37 °C.

NO Formation Assay. Nitric oxide production by the iNOS was measured spectrophotometrically by the conversion of oxyhemoglobin to methemoglobin as the increase in absorbance at 401 nm over time. Reaction mixtures contained 50 mM Hepes, pH 7.5, 100 μM NADPH, 0.003 mg/mL CaM, 1 mM EGTA, 100 μM L-arginine, and 5 μM oxyhemoglobin. Incubations were initiated by addition of the enzyme and were carried out for 30 min at 37 °C.

Fluorometric Assay for Protoporphyrin. The heme content of the iNOS samples was measured fluorometrically as described previously (*14*) by analyzing the emission spectrum (560−680 nm, excitation 410 nm) on a Perkin-Elmer MPF-66 fluorescence spectrophotometer. Samples (25 μL) boiled in 1 mL of 1 M oxalic acid for 30 min were examined. Freshly prepared heme solutions were used as standards.

SDS−PAGE. Incubations of the iNOS with ^{14}C-labeled inhibitors were treated with acetone to precipitate the protein, the suspensions were centrifuged, and the pellets were resuspended in 100 μL of Laemmli sample buffer (LSB), and 35 μL was applied to a 7.5% mini-slab-gels. SDS−PAGE was run at 30 mA constant current at 4 °C for 1−2 h. Samples from sucrose density gradients were analyzed without acetone precipitation by mixing with LSB and were boiled for 5 min before their application to the gels.

Western Blotting. The gels were transferred to a nitrocellulose membrane and probed with anti-iNOS antibodies (UBI). Anti-rabbit alkaline phosphatase conjugated goat IgGs were used as secondary antibodies, and the blots were developed by using nitro blue tetrazolium as a substrate for color detection. The blots were scanned, and their density was analyzed by computer using NIH Image 1.61 software (data not shown).

Sucrose Density Gradients. Incubations of the iNOS with inhibitors were conducted at 30 °C until activity was

undetectable in citrulline formation assay. Reaction mixtures were adjusted to contain 50 μM L-arginine and 50 μM BH_4 and were incubated for an additional 10 min at 37 °C. Portions (350 μL) were applied immediately to the top of continuous 5−20% sucrose density gradients containing 50 mM MOPS, pH 7.4, 150 mM NaCl, 1 mM EGTA, 1 mM DTT, 0.3% CHAPSO, and 10 μM BH_4. Gradients were run at 30 000 rpm for 18 h in a L5-75 Beckman Ultracentrifuge using a SW41 rotor. Fractions (375 μL) were collected using an ISCO density gradient fractionator, model 185. The fractions from the gradients were kept on ice, and portions were assayed for cytochrome *c* reductase activity, citrulline-forming activity, and heme fluorescence or were Western blot analyzed following 7.5% SDS−PAGE fractionation. Hemoglobin (5 mg/mL), catalase (20 mg/mL), and thyroglobulin (5 mg/mL) were used as sedimentation marker proteins for the sucrose gradient and were run in a separate tube.

HPLC Analysis. HPLC was run on a Partisil 5 μm ODS-3 (4.6 × 250 mm) HPLC column (Whatman) in an acetonitrile (60)/water (40)/TFA (0.1) solvent system as described previously (*15*). Samples for analysis were mixed with an equal volume of the column development solvent, and 100 μL was injected. The column was run at a flow rate of 1 mL/min and the effluent monitored at 398 nm (heme) and at 280 nm (protein). Fractions of 0.25 mL were collected and 100 μL portions counted for ^{14}C radioactivity.

Stoichiometry of ^{14}C-AG Labeling. Incubations were run in 30 mM Hepes, pH 7.5, 1 mM DTT, 1 mM EGTA, 100 μM NADPH, and 100 μM BH_4, with DE-purified homogeneous iNOS sample and were initiated by addition of ^{14}C-AG to a final concentration of 100 μM. Parallel incubation was adjusted to contain 10 mM L-arginine to determine the nonspecific labeling. Incubations were conducted at 30 °C for the time sufficient to completely inactivate NO-forming activity, as determined by NO formation assay. The free unreacted ^{14}C-AG was washed away with 50 mM HEPES, pH 7.5 by multiple concentrations and dilutions in Centricon 100 concentrator until no radioactivity was detected in the filtrate. The concentrated sample was assayed for protein and counted for ^{14}C radioactivity. The stoichiometry of ^{14}C-AG labeling is expressed as moles of ^{14}C-AG per moles of iNOS monomer.

Miscellaneous Procedures. The protein concentration was determined by Bradford (*16*) assay using bovine serum albumin as a standard.

RESULTS

Kinetic studies from our laboratory have established that AG is an iNOS-selective, mechanism-based inactivator (*9*). Similar studies conducted in our laboratory indicate that NIL produces a time and concentration dependent loss of the iNOS-catalyzed NO-forming activity that follows pseudo-first-order kinetics and occurs only under conditions that support catalytic activity, thus fulfilling many of the criteria for being a mechanism-based inactivator of NOS (unpublished results). Therefore, we were interested in determining the molecular mechanism by which each of the inhibitors inactivates the iNOS. Presuming AG and NIL to be mechanism-based inactivators, both need to be activated by the iNOS to their reactive intermediates that alter the functionality of the active site by covalent modification of the polypeptide chain or other active site structures. The two consecutive monooxygenation reactions catalyzed by iNOS (*17*) require the presence of two functional heme residues (*18*) at least one of which is capable of binding and activating molecular oxygen. The mechanism-based inactivator N^G-methyl-L-arginine has been shown by Olken et al. (*19*) to produce a loss of heme, establishing the precedent that mechanism-based inactivators of NOS may produce heme loss. Accordingly, we decided to explore whether AG or NIL act by altering the heme integrity at the active site of iNOS.

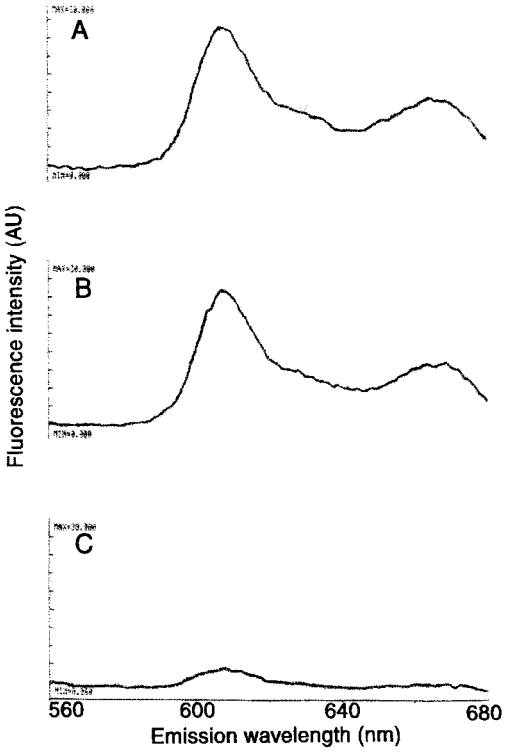

FIGURE 1: Fluorescence emission spectrum of the iNOS heme: (panel A) control iNOS; (panel B) AG-inactivated iNOS; (panel C) NIL-inactivated iNOS. Affinity-purified iNOS samples were incubated with AG or NIL for times sufficient to completely inactivate iNOS activity, as determined by citrulline formation assays. Samples were concentrated in a Centricon 30 device, and 25 μL aliquots of the concentrate were boiled in 1 M oxalic acid for 30 min. The emission spectrum was recorded at 410 nm excitation.

Analysis of the iNOS Heme. The fluorescence emission spectrum of iNOS was examined (Figure 1A) and displayed the characteristic heme protoporphyrin IX fluorescence with two major peaks at 606 and 662 nm (*20*). An identical spectrum was recorded after complete inactivation of the iNOS with AG (Figure 1B), suggesting that despite inactivation, the porphyrin ring remained intact. In contrast to this, an altered spectrum was observed after inactivation of the iNOS with NIL (Figure 1C). The fluorescence of the heme peaks at 606 and 662 nm disappeared following treatment, indicative of the loss of integrity of the heme porphyrin ring. This suggests that NIL inactivation may involve heme destruction and/or its loss from the active site.

We explored the possibility that the loss of heme integrity is the primary mechanism of NIL-induced inactivation by examining the time-dependent changes of heme fluorescence and catalytic activity in NIL-treated iNOS samples. In an

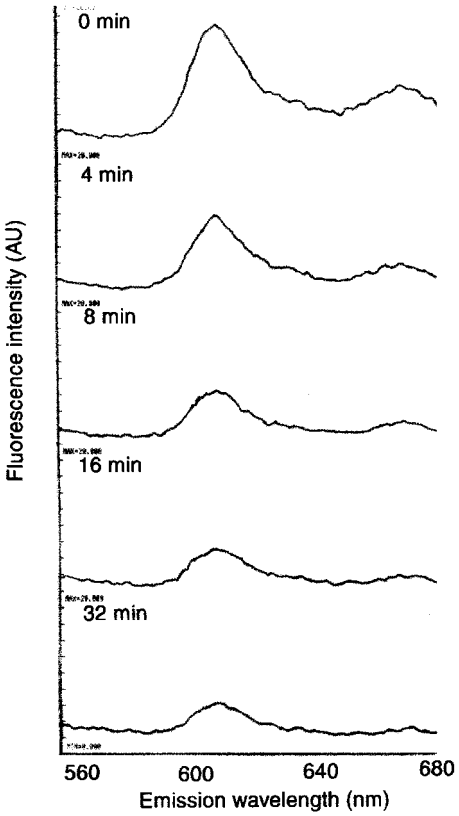

FIGURE 2: Effect of the iNOS preincubation with NIL on the heme fluorescence emission spectrum of iNOS. The affinity-purified iNOS sample was incubated with 5 μM NIL for 32 min at 37 °C. Aliquots of 25 μL were withdrawn at 0, 4, 8, 16, and 32 min postinitiation and boiled in 1 mL of 1 M oxalic acid for 30 min. The emission spectrum was recorded at 410 nm excitation for each time point.

initial study conducted at 5 μM NIL (Figure 2), incubation of iNOS under conditions that supported catalytic activity produced a loss of heme fluorescence that progressed with time. This observation at a single NIL concentration was extended by examining concurrently the time-dependent loss of heme fluorescence and iNOS-catalyzed NO-forming activity at three fixed concentrations of NIL (Figure 3). As measured in incubations containing 20 or 5 μM NIL, iNOS activity was completely inactivated within 15 min with a somewhat more rapid rate of inactivation being observed at 20 μM NIL. As measured at 2 μM NIL, inactivation of NO-forming activity declined more slowly but was approximately 90% complete within 30 min. Similarly, as measured in incubations containing 20 or 5 μM NIL, heme destruction occurred with a time course similar to the decline of catalytic activity, but in contrast to the complete loss of catalytic activity, the destruction of heme fluorescence was incomplete, with a residual heme fluorescence approximately 30% of its initial value. As measured in incubations containing 2 μM NIL, the decline of heme fluorescence was slower, as had been noted for the decline of catalytic activity, with a heme fluorescence 40% of its initial value achieved by 30 min. A control incubation containing iNOS without NIL, lost less than 10% of both NO-forming activity and heme fluorescence (data not shown). Thus, both NO-forming activity and heme fluorescence declined with a similar time and concentration dependence in NIL-treated samples; however, despite complete enzyme inactivation, approximately 30% of heme residues appeared refractory to NIL treatment.

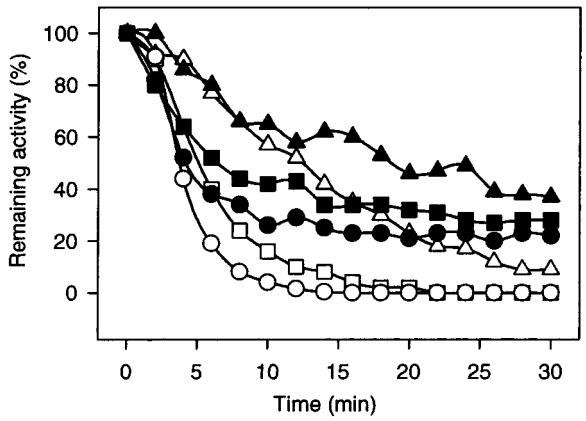

FIGURE 3: Effect of increasing NIL concentration on time-dependent changes of iNOS activity and heme fluorescence. Affinity-purified iNOS was incubated with 2 μM (triangles), 5 μM (squares), and 20 μM (circles) NIL for 30 min at 37 °C as described in Materials and Methods. Aliquots were withdrawn every 2 min and were assayed for NO-forming activity (open symbols) and heme fluorescence (closed symbols). The data are presented as a percentage of NO-forming activity or heme fluorescence remaining at the specified time as compared with the zero time values.

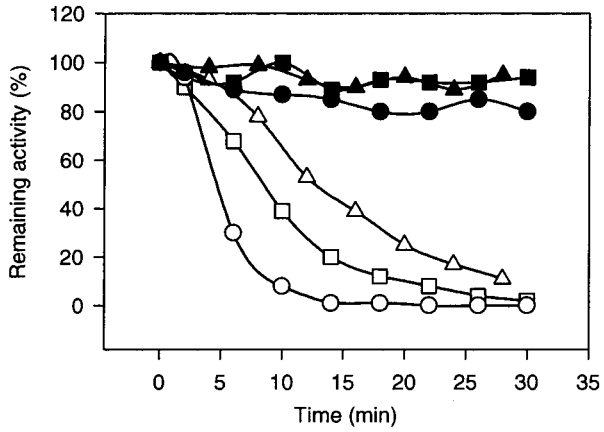

FIGURE 4: Effect of increasing AG concentration on time-dependent changes of iNOS activity and heme fluorescence. Affinity-purified iNOS was incubated with 100 μM (triangles), 250 μM (squares), and 500 μM (circles) AG for 30 min at 37 °C. Aliquots were withdrawn every 2 min and were assayed for NO-forming activity (open symbols) and heme fluorescence (closed symbols). The data are presented as a percentage of NO-forming activity or heme fluorescence remaining at the specified time as compared with the zero time values.

In a parallel experiment, the loss of NO formation and heme fluorescence during the iNOS incubation with AG was examined (Figure 4). Neither increasing AG concentration nor prolonging the time of incubation had any effect on the heme fluorescence, although the NO-forming activity was completely lost. Thus, even at 500 μM AG, more than 80% of heme fluorescence was preserved after a 30 min incubation period, despite a more than 90% loss of the NO-forming activity during the first 10 min of incubation.

Fractionation of the NIL- and AG-Treated iNOS by Sucrose Density Gradient Centrifugation. To explain the discrepancy between the complete loss of NO-forming activity and only about 70% decrease in heme fluorescence, we explored two different, but not mutually exclusive hypotheses. First, NIL as a mechanism-based inhibitor

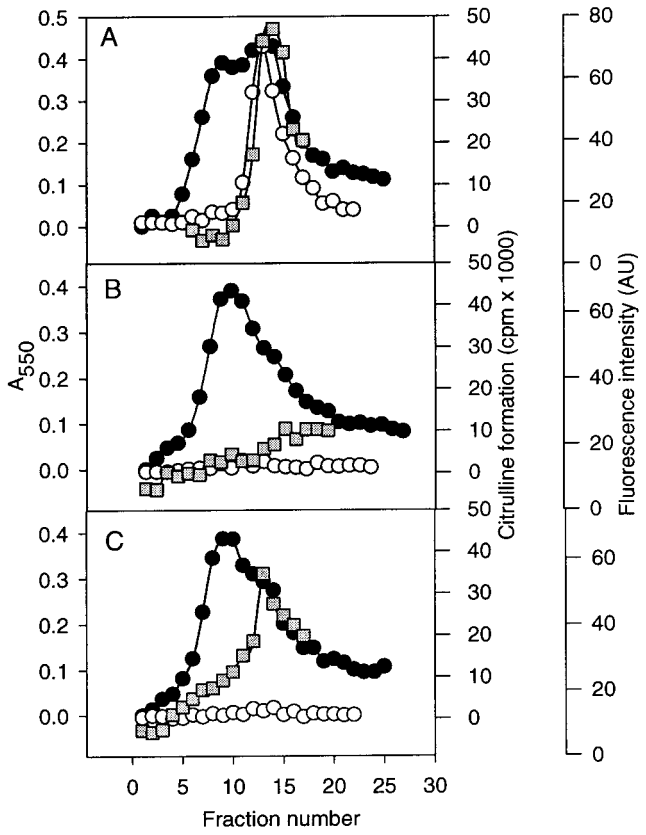

FIGURE 5: Analysis of the effects of NIL and AG treatment on the iNOS dimeric and monomeric forms fractionated by sucrose density gradient centrifugation: (panel A) iNOS control; (panel B) iNOS + 5 μM NIL; (panel C) iNOS + 50 μM AG. The control and drug-inactivated iNOS samples were run on the continuous 5−20% sucrose density gradients. Fractions of 375 μL were collected and assayed for cytochrome *c* reductase activity (closed circles), citrulline-forming activity (open circles), and heme fluorescence (squares). The figure is a representative of three different experiments performed under the same conditions.

inactivates only the iNOS dimeric population, which is catalytically competent to reduce oxygen and thus is able to process NIL into its reactive intermediate. Therefore, the residual heme fluorescence refractory to NIL treatment may reflect a heme pool bound to iNOS monomers that have not been assembled into dimers and thus are catalytically incompetent to activate NIL into its reactive intermediate. Alternately, each iNOS dimer requires two heme residues to support catalytic activity and NIL inactivation may involve the destruction of only one heme at each dimeric active site. Alternately, both considerations may apply. We used the approach of fractionating the untreated and drug-inactivated iNOS into their monomeric and dimeric forms using sucrose density gradients. Following treatment and fractionation (Figure 5), each of the gradient fractions was assayed for heme fluorescence, for cytochrome *c* reductase activity (an activity possessed by both monomers and dimers), and for citrulline-forming activity (an activity possessed only by iNOS dimers).

The untreated iNOS (Figure 5A) displayed two peaks of the cytochrome *c* reductase activity (fractions 8 and 12) both of which were attributable to the iNOS, as evidenced by the iNOS cross-reactivity in the gradient fractions 7 through 14 (Figure 6). The first peak (fraction 8) represented the iNOS monomers, whereas the second peak (fraction 12) possessed

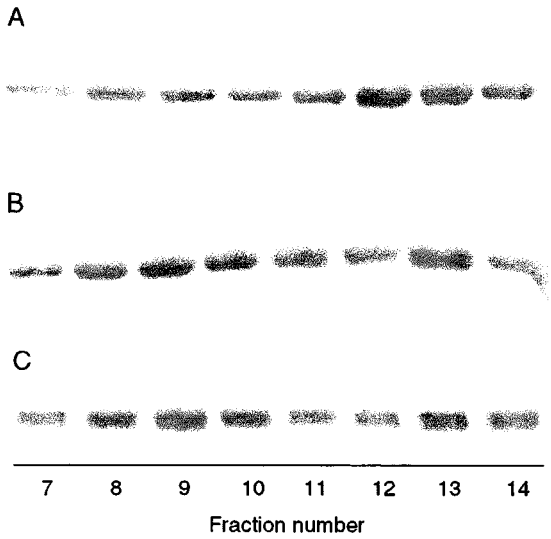

FIGURE 6: Western blot of the sucrose density gradient fractions of the control and drug-inactivated iNOS. Fractions 7−14 from the sucrose density gradients of the control iNOS (A), NIL-inactivated iNOS (B), and AG-inactivated iNOS (C) were concentrated, run on a 7.5% SDS−PAGE, transferred to nitrocellulose membrane, and probed with the anti-iNOS antibodies. The figure is a representative of three different experiments performed under the same conditions.

citrulline-forming activity and thus corresponded to the iNOS dimers. This dimer peak contained virtually the entire heme pool. No heme fluorescence was observed associated with the iNOS monomeric fractions. NIL inhibition was accompanied by the complete loss of the citrulline-forming activity of the dimer peak as well as dramatically diminished heme fluorescence (Figure 5B). A small but identifiable heme fluorescence was retained by the dimeric iNOS population, suggesting that the heme fluorescence remaining after NIL treatment represents the dimeric iNOS heme that has not been destroyed by the inactivator. Similarly, the AG-inactivated iNOS fractionated into the monomeric and dimeric population without any detectable citrulline-forming activity. Interestingly, the fractions containing the AG-inactivated dimeric iNOS were easily identifiable by the fluorescence of their heme pool (Figure 5C). The major heme fluorescence peak appeared in fraction 12, which contained the dimeric iNOS. In addition, some increased heme fluorescence was observed in the monomeric iNOS fractions 6 through 10 when compared with the gradient fractions from the untreated iNOS sample.

Following the treatment of the iNOS with NIL or AG the relative peak heights of cytochrome *c* reductase activity of the monomeric and dimeric fractions changed so that the peak associated with the dimeric iNOS (fraction 12) was considerably reduced, suggesting that the inactivated dimers at least in part dissociate into monomers. The Western blots of the untreated and drug-inactivated iNOS samples assayed in Figure 5 are presented in Figure 6 and show that, after inactivation, especially in the case of NIL, the monomer/dimer equilibrium changed and shifted toward the prevalence of the iNOS monomers over the dimers. Nevertheless, in each case, a certain fraction of the dimers still was preserved after treatment with NIL or AG despite the complete loss of NO-forming activity.

Incubation of the iNOS with ^{14}C-Labeled NIL and AG. The majority of mechanism-based inhibitors act through

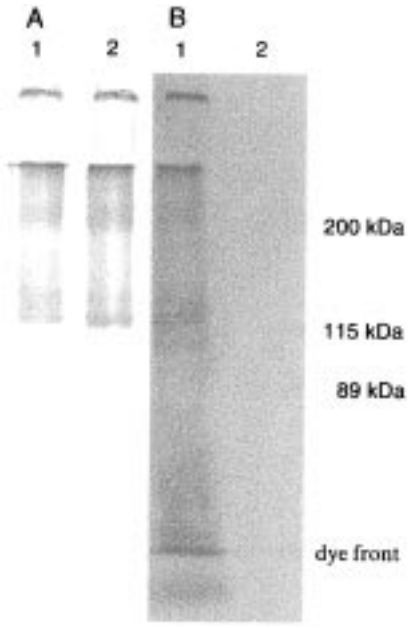

FIGURE 7: Western blot and autoradiogram of the ^{14}C−NIL (300 mCi/mmol) and ^{14}C-AG (56 mCi/mmol) inactivated iNOS: (panel A) Western blot; (panel B) autoradiogram of the Western blot; (lane 1), iNOS + ^{14}C-AG; (lane 2) iNOS + ^{14}C-NIL. Affinity-purified iNOS samples were incubated with 5 μM ^{14}C-NIL and 50 μM ^{14}C-AG for the time sufficient to completely inactivate iNOS, as determined by the enzyme's ability to produce NO. Acetone-precipitated protein was dissolved in 100 μL of LSB, and 35 μL of the resulting solution was run on a 7.5% SDS−PAGE, transferred to a nitrocellulose membrane, and probed with the anti-iNOS antibodies. The Western blot was exposed for 10 days.

covalent modification of the enzyme's active site by incorporating the inhibitor's backbone or a part of it, into the polypeptide chain or other active site structures (e.g., heme). Therefore, we decided to use ^{14}C-labeled AG and NIL to determine whether any of the counts are incorporated into the iNOS protein. The iNOS was incubated with ^{14}C-NIL or ^{14}C-AG followed by acetone precipitation of the protein, which was resolved on a 7.5% SDS−PAGE. Interestingly, no ^{14}C counts associated with the acetone-precipitated iNOS protein were detected after complete inactivation with NIL. The Western blot (panel A) and autoradiogram (panel B) shown in Figure 7 (lane 2) support this observation. At the same time, incubations of the iNOS with ^{14}C-AG resulted in acetone precipitation of ^{14}C-radioactivity (Figure 7B, lane 1), which resolved into radioactive bands of high molecular weight and low molecular weight structures that migrated with or immediately in front of the running buffer on a 7.5% SDS−PAGE. The identity of the high molecular weight bands with an apparent molecular weight of 130 000 was confirmed by the Western blot (Figure 7A) to be the iNOS protein. Additional higher molecular weight bands appeared to be the iNOS aggregates "hung up" at the buffer−sample gel and sample gel−running gel interfaces, as evidenced by their cross-reactivity with iNOS antibody. These aggregates contained "covalently-associated" radioactivity only in the AG-treated sample. The migration pattern of the lower molecular weight structure(s) resembled that of free heme when used as a standard. We next used HPLC analysis to clarify the identity of the radioactively labeled lower molecular weight structure(s).

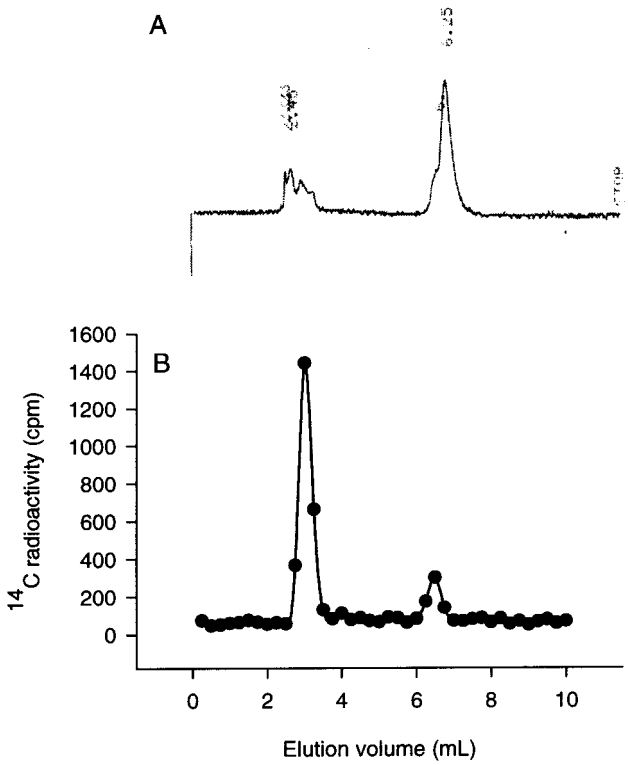

FIGURE 8: HPLC of the ^{14}C-AG-inactivated iNOS: (panel A) HPLC trace; (panel B) ^{14}C radioactivity of the collected fractions. The affinity-purified iNOS sample was treated with ^{14}C-AG for the time sufficient to completely inactivate iNOS, as determined by the enzyme's ability to produce NO. Free ^{14}C-aminoguanidine was washed out by multiple concentrations in a Centricon 30 device, and the concentrated iNOS sample was run on HPLC in an acetonitrile/water/TFA system on a Whatman Partisil 5 ODS-3 column at a flow rate of 1 mL/min, detector at 398 nm. Fractions of 250 μL were collected, and 100 μL was counted for ^{14}C radioactivity.

HPLC Analysis of the ^{14}C-AG Inactivated iNOS. The labeled iNOS was fractionated by HPLC in an acetonitrile/water/TFA solvent system and the effluent was monitored for protein at 280 nm and for the heme absorbance at 398 nm (Figure 8). Two major radioactive peaks were detected after counting the fractions collected during the HPLC run. The first peak that retained most of the ^{14}C counts eluted at 2.4 min with the major protein peak, whereas the smaller radioactive peak had a retention time of 6.26 min and an absorbance of 398 nm characteristic of a porphyrin and was identified as a protein-dissociable free heme by the near identity of its retention time with that of the hemoglobin-derived free "heme" when run as a standard. Some of the heme might have remained associated with the protein, as evidenced by the small peak of 398 nm absorbance of the protein peak that eluted at 2.4 min.

The radioactive peak associated with the protein was run on a 7.5% SDS−PAGE to resolve the proteins. The Western blot and autoradiogram in Figure 9 show the major radioactive protein band that corresponds in migration to the iNOS protein, as identified by its cross-reactivity with the anti-iNOS antibodies.

The stoichiometry of the iNOS protein labeling by ^{14}C-AG was determined by using a homogeneous sample of the iNOS. In the presence of NADPH and BH_4 the stoichiometry of labeling was calculated to be 1.93 mol of ^{14}C-AG/

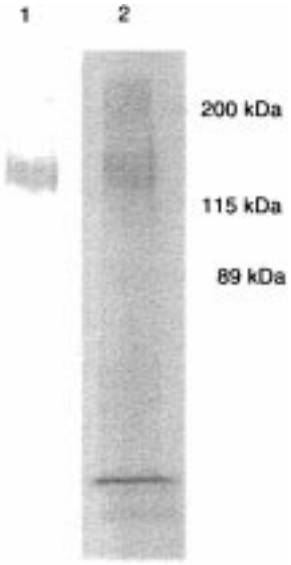

FIGURE 9: Western blot and autoradiogram of the ^{14}C-AG-labeled iNOS fractionated by HPLC: (lane 1) Western blot; (lane 2) autoradiogram of the Western blot. ^{14}C-labeled protein from the HPLC fractions 11 through 14 was precipitated with acetone and resuspended in 100 μL of LSB, and 35 μL was run on a 7.5% SDS−PAGE, transferred to nitrocellulose, and probed with anti-iNOS antibodies. The Western blot was exposed for 3 weeks.

mol of the iNOS monomer. In a parallel incubation that contained 10 mM L-arginine, the stoichiometry of labeling approached 1.3 mol of ^{14}C-AG/mol of the iNOS monomer, which gives a number for specific labeling to be about 0.63 mol of ^{14}C-AG/mol of the iNOS monomer.

DISCUSSION

Cytochrome P-450 enzymes have been extensively used in the studies of mechanism-based enzyme inactivators (*21*). These studies established three major pathways for the mechanism-based destruction of heme-containing oxidative enzymes. All of the mechanisms theoretically can be applied to the iNOS inactivation by mechanism-based inactivators by taking into account that NOS isozymes are cytochrome P-450-like monooxygenase systems and contain a P-450-like heme residue at their active site, which is required for catalysis. The first pathway leads to the covalent modification of the heme residue at the active site (*22*), resulting in the formation of a heme adduct incapable of participating in catalytic activation of oxygen and is well documented for terminal olefins, terminal acetylenes, dihydropyridines, and dihydroquinolines as cytochrome P-450 inhibitors (*23*−*25*). Alignment of mechanism-based inhibitors such as NIL and AG at the iNOS active site is competitive versus the L-arginine substrate (*9*, unpublished results) and occurs in close proximity to the heme residue that is located next to the arginine binding site and should be positioned close to the guanidino group of arginine for successive hydroxylation (*26*). Thus, the reactive oxygenated intermediates of NIL and AG are generated in close proximity to the heme residue and can primarily attack and covalently modify it, incorporating the inactivator's backbone, or a part of it, into the heme residue.

The second pathway proceeds through covalent modification of a nucleophilic amino acid residue that projects into the active site and is documented for parathion, and chloramphenicol (*27*). The third pathway results in the covalent linkage of the heme residue to protein (*28*). The above-mentioned major pathways followed by mechanism-based inactivators are not mutually exclusive, as shown for the cytochromes P-450. Thus, covalent modification of the heme residue may be accompanied by the covalent modification of the protein at the active site or covalent linkage of heme to the polypeptide chain as well (*29*).

Structurally, NIL and AG are quite different from one another and based on our results seem to follow different pathways by which they produce the inhibition of iNOS activity. Thus, our data support the conclusion that the primary pathway of iNOS inactivation by NIL targets the heme residue at the active site and leads to its modification. The reactive intermediate generated from NIL by iNOS must be positioned in very close proximity to the heme residue and attacks it, generating a heme adduct that is altered structurally in such a way as to eliminate its fluorescence spectrum and probably its affinity for protein-binding. This conclusion is evidenced by the disappearance of heme fluorescence during NIL incubation with the iNOS (Figure 2). The loss of heme fluorescence implies that the integrity of the tetrapyrrolic porphyrin structure is compromised in such a way that it is either destroyed or the heme adduct generated is destabilized such that it cannot survive the treatment with oxalic acid during the assay conditions. It is well documented for the cytochromes P-450 that some mechanism-based inactivators lead to the formation of stable heme adducts that preserve the fluorescence of the porphyrin ring while other inactivators such as peroxide, halocarbons, allenes, cyclopropylamines, and benzothiadiazoles produce intermediates that result in the loss of porphyrin fluorescence (*30*). The observation that the loss of heme fluorescence is a time- and concentration-dependent process occurring concomitantly with the loss of NO-forming activity (Figure 3) suggests that these NIL-induced changes occur by a mechanism-based process.

The identity of the product(s) generated from the iNOS heme as a result of NIL attack was not determined. The destruction of the porphyrin ring in many cases leads to the formation of pyrrole and dipyrrole structures that are difficult to detect and require the use of generous quantities of the hemoprotein. Incubations of the iNOS with radioactively labeled NIL provided evidence that the products generated in the course of inactivation do not associate covalently with the iNOS protein, as no counts were detected in the protein precipitate. Therefore, we conclude that the porphyrin adducts being formed are not getting covalently attached to the polypeptide chain, as has been observed for some cytochrome P-450 mechanism-based inactivators (*31*).

The complete loss of NO-forming activity following NIL treatment was never accompanied by a complete loss of heme fluorescence. Examination of our iNOS preparation by sucrose density gradient centrifugation revealed that all of the heme present in our preparation was associated with the dimeric form of iNOS. Further, following NIL treatment, a complete loss of dimer catalytic activity was associated with a partial loss of dimer-associated heme. Complementation analysis of iNOS mutants has revealed that dimerization of the iNOS monomers each containing a heme residue is necessary to form an active site catalytically competent to synthesize NO (*18*). Therefore, NIL inactivation may

involve the destruction of only one heme residue, which is sufficient for the complete loss of NO-forming activity but which retains initially one "undamaged" heme residue.

As a consequence of this NIL-dependent heme alteration, the inactivated iNOS dimers have decreased dimeric stability and partially disassemble into monomers. This is supported both by Western blot analysis of the sucrose density gradient fractions, which shows a shift in the monomer/dimer equilibrium toward prevalence of the iNOS monomers, and by increased monomeric cytochrome *c* reductase activity. This result is not surprising, as the formation of dimers is promoted by the presence of heme as well as by the BH_4 cofactor and amino acid substrate (*32*). Although it is primarily BH_4 and L-arginine that generate the formation of the stable iNOS dimers, the presence of heme is a necessary requirement for the formation of dimers (*33*). Therefore, "destruction" of one of two heme residues at the iNOS active site appears to promote subunit dissociation and generation of the iNOS monomers. The residual heme residue may dissociate from the monomer. The dissociated heme, being neither monomer- nor dimer-associated, would fractionate at the top of the sucrose gradient.

A different mechanism of the iNOS inhibition is produced by AG. The fluorescence of the iNOS heme is preserved, suggesting that the porphyrin ring is not destroyed during or as a result of inactivation, and the heme remains iNOS-associated, as evidenced by the retention of heme fluorescence with iNOS on sucrose density gradients (Figure 5).

When iNOS is incubated with radioactively labeled AG, the ^{14}C counts are incorporated into the iNOS protein and low molecular weight structures that migrate in the SDS−PAGE similarly to free heme and can be identified by HPLC as a protein-dissociable free heme adduct by its retention time and absorbance. Thus, the results suggest that AG follows multiple inactivation pathways that include covalent modification of both the iNOS protein chain and heme residue. Which of these two outcomes is the "decisive" pathway for the iNOS inactivation is not known. The studies of P-450 enzymes suggest that protein modification is much less important than heme derivatization and can occur without significant activity loss unless the porphyrin ring is covalently modified along with the protein (*34*). The stoichiometric studies of the iNOS protein labeling by ^{14}C-AG indicated that 0.63 mol of ^{14}C-AG covalently labeled 1 mol of the iNOS monomer. Thus, the stoichiometry approached a value of 1 mol of ^{14}C-AG/mol of the iNOS dimer. This stoichiometry supports a specific adduct formation rather than widespread nonspecific labeling occurring at multiple sites.

In following multiple pathways of the iNOS inactivation, AG appears similar to NMA, which is the only other NOS mechanism-based inactivator that has been studied, and proceeds through multiple pathways as reported by Olken et al. (*19*). These include heme loss as detected by HPLC analysis as a major pathway and additional protein plus possible cofactor covalent modification. Nevertheless, the destruction of the heme residue was considered to be the primary pathway of the mechanism-based inactivation, similarly to the one produced by NIL. The differences in the NMA, NIL, and AG patterns of inactivation can be attributed to the different structural features of these inactivators and their positioning at the active site. Thus, both NMA and NIL are amino acid derivatives similar in size to the L-arginine molecule and bind at the L-arginine binding domain, gaining access to the heme pocket only with their methyl or iminoethyl group probably oriented toward the distal heme ligand at the sixth coordination position, as proposed for the L-arginine guanidino group. As the position of the amino acid backbone is fixed, the reactive intermediates generated probably project directly at the heme, thus attacking it and leading to its destruction. On the other hand, AG is a hydrazine molecule much smaller in size, 3.8×4.3 Å ($X \times Y$) (*35*), which can easily fit into the active site heme pocket and bind at the site that is occupied normally by the L-arginine guanidino group. Thus, the whole AG molecule will be positioned in close proximity to the heme residue. Its diminished size may permit more flexibility in attacking multiple sites.

Thus, we have shown that two structurally different iNOS selective mechanism-based inactivators follow different chemical and molecular pathways by which they inactivate the iNOS isoform. We are currently examining NIL and AG with respect to the nNOS isoform, an isoform for which they are far less efficient as inactivators. It will be interesting whether these inactivators will follow identical pathways in the case of a different NOS isoform. The knowledge of the exact molecular pathways of inactivation for each isoform may aid in identification of structural features that are crucial for selective inhibition of the NOS isozymes and lead to the development of new compounds with yet enhanced specificity.

REFERENCES

1. Kwon, N. S., Nathan, C. F., Gilker, C., Griffith, O. W., Matthews, D. E., and Stuehr, D. J. (1990) *J. Biol. Chem. 265*, 13442−13445.
2. Masters, B. S. S., McMillan, K., Sheta, E. A., Nishimura, J. S., Roman, L. J., and Martasek, P. (1996) *FASEB J. 10*, 552−558.
3. Stuehr, D. J. (1997) *Annu. Rev. Pharmacol. Toxicol. 37*, 339−359.
4. MacMicking, J., Xie, Q., and Nathan, C. (1997) *Annu. Rev. Immunol. 15*, 323−350.
5. Moncada, S. and Higgs, E. A. (1995) *FASEB J. 9*, 1319−1330.
6. Connor, J. R., Manning, P. T., Settle, S. L., Moore, W. M., Jerome, G. M., Webber, R. K., Tjoeng, F. S., and Currie, M. G. (1995) *Eur. J. Pharm. 273*, 15−24.
7. Zhao, W., Tilton, R. G., Corbett, J. A., McDaniel, M. L., Misko, T. P., Williamson, J. R., Cross, A. H., and Hickey, W. F. (1996) *J. Neuroimmunol. 64*, 123−133.
8. Moore, W. M., Webber, R. K., Jerome, G. M., Tjoeng, F. S., Misko, T. P., and Currie, M. G. (1994) *J. Med. Chem. 37*, 3886−3888.
9. Wolff, D. J., and Lubeskie, A. (1995) *Arch. Biochem. Biophys. 316*, 290−301.
10. Silverman, R. B. (1988) *Mechanism-based Enzyme Inactivation: Chemistry and Enzymology* Vol. 1, pp 1−27, CRC Press, Boca Raton, FL.
11. Osawa, Y. and Pohl, L. R. (1989) *Chem. Res. Tox. 2*, 131−141.
12. Wolff, D. J. and Gribin, B. J. (1994) *Arch. Biochem. Biophys. 311*, 293−299.
13. Wolff, D. J. and Datto, G. A. (1992) *Biochem. J. 285*, 201−206.
14. Morrison, G. R. (1965) *Anal. Chem. 37*, 1124−1126.
15. Mayer, B., Klatt, P., Harteneck, C., List, B. M., Werner, E. R., and Schmidt, K. (1996) in *Nitric Oxide Synthase: Characterization and Functional Analysis* (Maines, M. D., Ed.) pp 130−139, Academic Press, San Diego, CA.

16. Bradford, M. M. (1976) *Anal. Biochem. 72*, 248−254.
17. Marletta, M. A. (1993) *J. Biol. Chem. 268*, 12231−12234.
18. Xie, Q., Leung, M., Fuortes, M., Sassa, S., and Nathan, C. (1996) *Proc. Natl. Acad. Sci. U.S.A. 93*, 4891−4896.
19. Olken, N. M., Osawa, Y., and Marletta, M. A. (1994) *Biochemistry 33*, 14784−14791.
20. Cho, H. J., Martin, E., Xie, Q., Sassa, S., and Nathan, C. (1995) *Proc. Natl. Acad. Sci. U.S.A. 92*, 11514−11518.
21. Walsh, C. T. (1984) *Annu. Rev. Biochem. 53*, 493−535.
22. Ortiz de Montellano, P. R. (1990) *Pharm. Therap. 48*, 95−120.
23. Ortiz de Montellano, P. R., and Correia, M. A. (1983) *Annu. Rev. Pharmacol. Toxicol. 23*, 481−503.
24. Ortiz de Montellano, P. R., and Komives, E. A. (1985) *J. Biol. Chem. 260*, 3330−3336.
25. De Matteis, F., Hollands, C., Gibbs, A. H., de Sa, N., and Rizzardini, M. (1982) *FEBS Lett. 145*, 87−92.
26. Sennequier, N., and Stuehr, D. J. (1996) *Biochemistry 35*, 5883−5892.
27. Halpert, J. (1981) *Biochem. Pharmacol. 30*, 875−881.
28. Davies, H. W., Satoh, H., Schulick, R. D., and Pohl, L. R. (1985) *Biochem. Pharmacol. 34*, 3203−3206.
29. He, K., He, Y. A., Szklarz, G. D., Halpert, J. R., and Correia, M. A. (1996) *J. Biol. Chem. 271*, 25864−25872.
30. Manno, M., King, L. J., de Matteis, F. (1989) *Xenobiot. 19*, 1023−1035.
31. Guengerich, P. F. (1978) *Biochemistry 17*, 3633−3639.
32. Baek, K. J., Thiel, B. A., Lucas, S., and Stuehr, D. J. (1993) *J. Biol. Chem. 268*, 21120−21129.
33. Albakri, Q. A., and Stuehr, D. J. (1996) *J. Biol. Chem. 271*, 5414−5421.
34. Ortiz de Montellano, P. R., and Reich N. O. (1986) in *Cytochrome P-450: Structure, Mechanism, and Biochemistry* (Ortiz de Montellano, P. R., Ed.) pp 273−314, Plenum Press, New York.
35. Berka, V., Chen, P.-F., and Tsai, A.-L. (1996) *J. Biol. Chem. 271*, 33293−33300.

BI972065T